



**TONSTEIN AND BENTONITE CORRELATIONS IN NORTHEAST BRITISH COLUMBIA  
(930, P, I; 94A)**

By W. E. Kilby

**INTRODUCTION**

Examination and correlation of tonsteins and bentonites was continued in northeastern British Columbia during the 1984 field season. Correlation distances were doubled for several of the previously identified tonstein horizons. Samples were collected for radiometric age dating. Several formation contacts were examined on a regional scale with respect to tonstein and bentonite horizons. Chemical data became available for 58 samples. Preliminary statistical analysis of this data was encouraging for correlation purposes. Mineralogical (XRD) results also appear to hold promise as a correlation tool.

**REGIONAL CORRELATIONS**

Volcanic ash falls, by their nature, cover large areas. Given the proper low energy depositional environment the resultant tonsteins and bentonites can be present over large distances. Three previously described zones (Kilby, 1984) were examined and have had their correlatable distances considerably extended. Ash bands in the Hulcross, Moosebar, and Gething Formations were used to gain an understanding of the diachronous nature of several formational contacts. A series of sections through the various horizons is presented below, the areal and stratigraphic positions of these sections are given on Figures 90 and 91.

**HULCROSS**

Prominent bentonite bands in the lower Hulcross Formation are exposed on the edge of Highway 29 along the Peace River east of Hudson's Hope; one 40-metre section in this area contained 17 bentonite horizons. A bentonite band located at the junction of Farrel Creek and the Peace River was sampled for radiometric age dating. This sample is presently undergoing analysis at the University of Alberta. A borehole drilled near this position encountered four prominent bentonite bands in the lower Hulcross. Examination of geophysical logs through this interval at widely spaced locations showed these four bands to be continuous over a considerable distance. Figure 92 is a display of geophysical logs from three widely spaced holes illustrating the relationship between the isochronous bentonite bands and the diachronous Hulcross-Gates contact. Several of these horizons were sampled and the correlation will be tested as chemical and mineralogical data become available. Examination of the

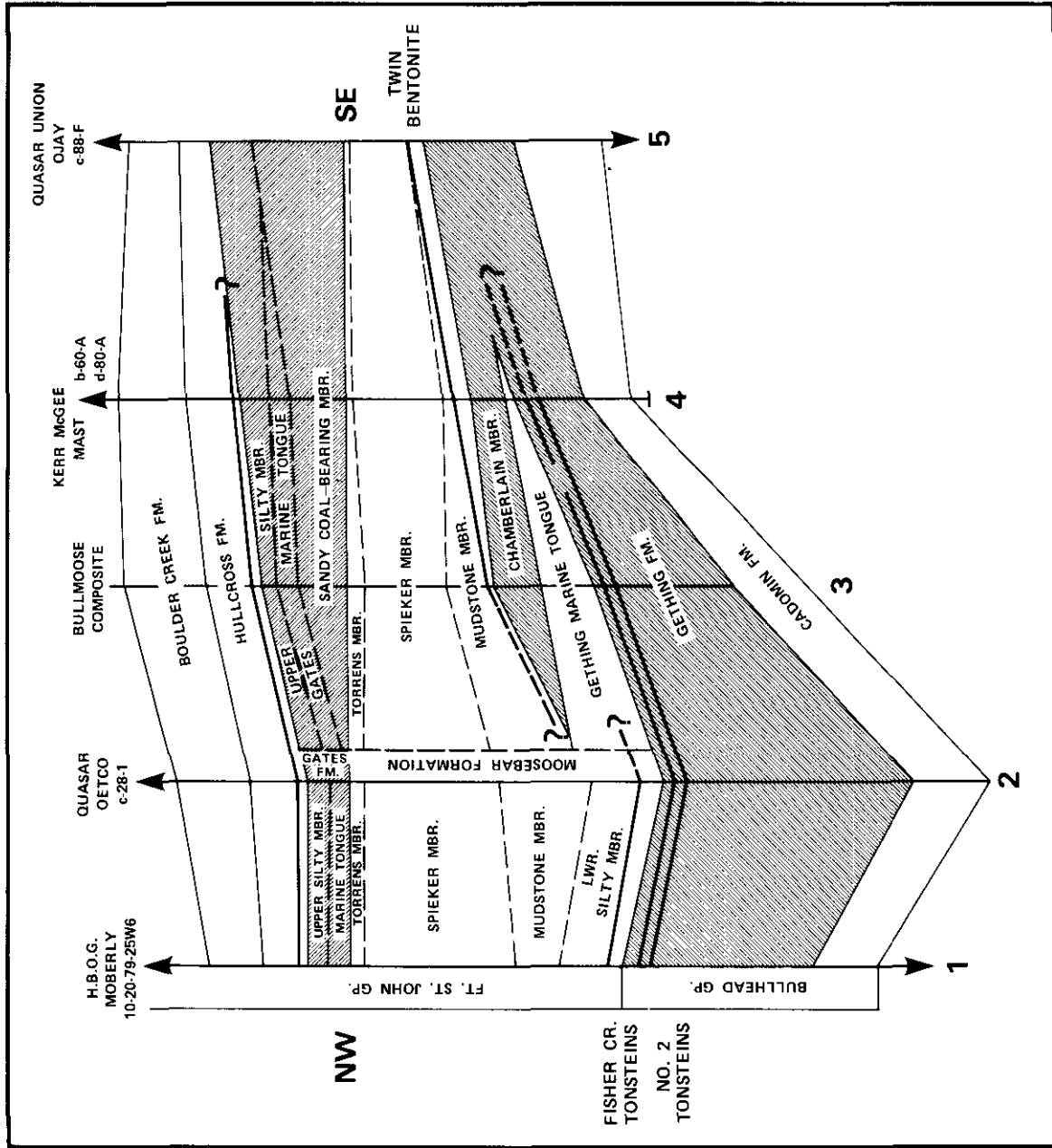


Figure 91. Schematic regional stratigraphic section illustrating the position and extent of major ash horizons examined in this study (modified after Duff and Gilchrist, 1981). Section position given on Figure 90.

sections show that at the time the lowest of the four ash bands was being deposited marine conditions had existed for a considerable time in the area of hole number 1 to the north, but in the area of hole number 3, coal swamp facies had just been replaced by marine sedimentation. The thickness of the intervening mudstone suggests that sedimentation rates appear almost constant over the length of this section during the time encompassed by these four bands.

#### MOOSEBAR

Bentonite horizons have previously been recognized in the Moosebar Formation from Peace River to the Grande Cache area of Alberta. Duff and Gilchrist (1981) correlated two prominent bands in the Bullmoose-Sukunka area. Two prominent bentonites have been used by workers in the Monkman area to sort out structural problems. A series of bentonites have been correlated in the Goodrich-Pine Pass area and a persistent series of thin bentonites are present along the Peace River (Kilby and Oppelt, this volume).

In the Peace River area a series of up to four bentonite bands are located about 10 metres above the Gething-Moosebar contact, or Bluesky (N) unit. These horizons have been traced more than 100 kilometres in an east-west direction (Kilby and Oppelt, this volume, *see* Fig. 80). A marked decrease occurs in the stratigraphic distance between these bentonites and the top of the Gething Formation in a westerly direction. In the west in borehole 1, the bentonites are in contact with siltstones, possibly of the Gething Formation, while to the east they are well above the Gething Formation. This coarser grained material, if not Gething Formation strata, at least suggests proximity to a shoreline or sediment source. A relatively constant thickness between the bentonite and Gething Formation is present from boreholes 2 to 23 while over, but from boreholes 13 to 14 a similar distance, the interval thickness quadruples. This significant thickness increase and the decrease in coal content in the underlying Gething Formation suggest that this area coincided with a break in facies in late Gething time.

In the Sukunka River to Belcourt Creek area two prominent bentonite horizons occur in the lower Moosebar Formation. These bentonites, referred to as the Twin Bentonites (Kilby, 1984), have been correlated over a distance of nearly 100 kilometres (Fig. 93) and the correlation is open at both ends. Figure 93 contains three borehole geophysical logs of these bentonites and the Moosebar-Gething contact. The constant thickness between the bands suggests a constant sedimentation rate over the area at the time of the ash falls. Also apparent is convergence of the bentonites and the Gething Formation in a northward direction. This relationship implies that coal swamps were present in the Sukunka area while marine Moosebar sedimentation was occurring to the south. As it is generally accepted that the Clearwater Sea transgressed in a southerly direction there must have been an embayment south of Sukunka or

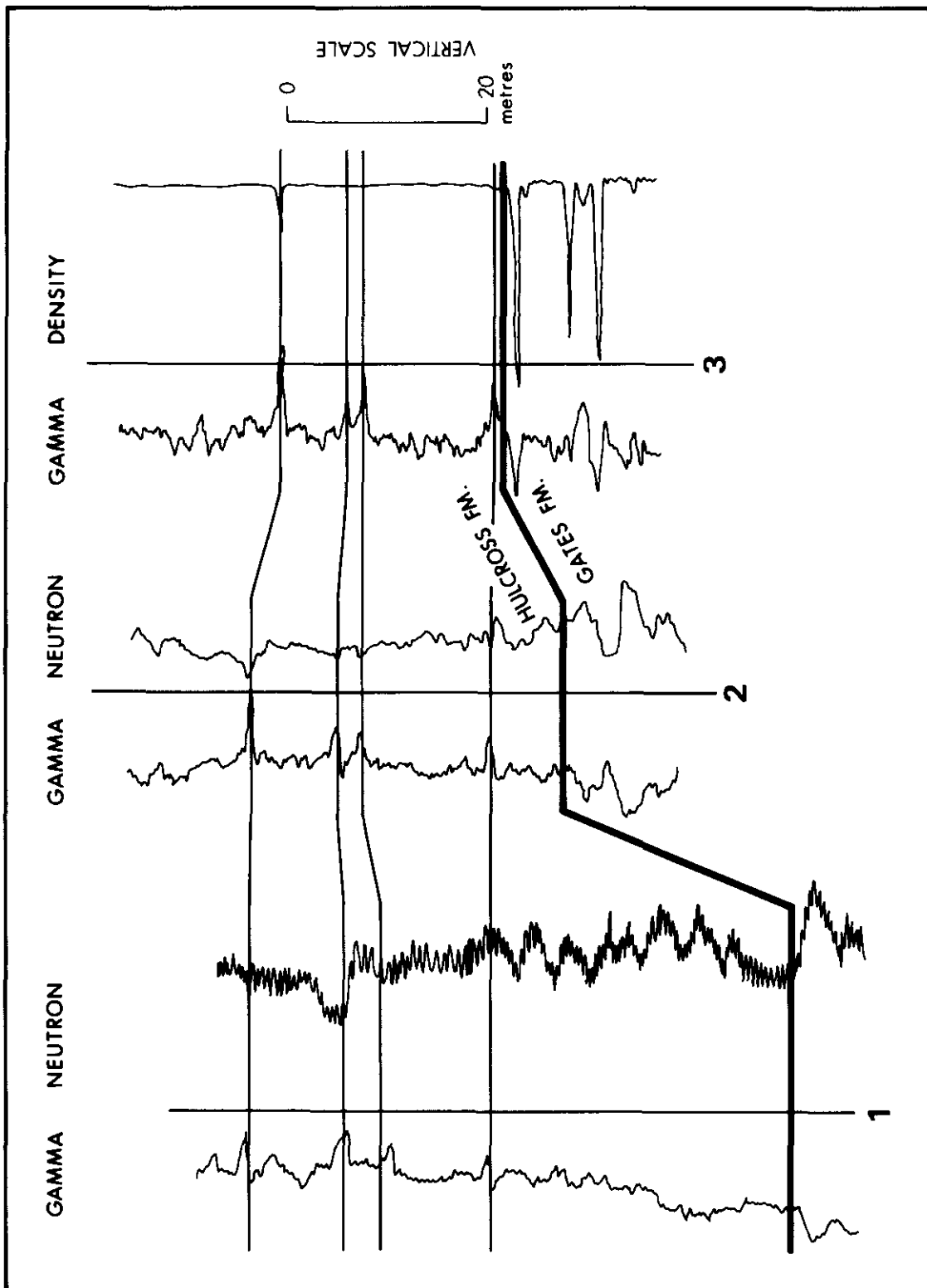


Figure 92. Bentonites in the lower Hulcross Formation. Bentonites appear as strong gamma responses (deflections to the right). See Figure 90 for location.

alternatively the Sukunka area formed a projection seaward (eastward), possibly in the form of a delta, during the early phases of the marine transgression. Duff and Gilchrist (1981) tentatively correlated these bentonite horizons with two bentonites in the Peace River area. This is a considerable distance with no intermediate data locations to reinforce the interpretation therefore this correlation remains questionable at this time.

In the Goodrich area, between the Pine River and Brazion Creek, a series of prominent bentonite horizons occur within the lower 50 metres of the Moosebar Formation. These bands have been used by company workers in the area and are traceable over a considerable distance. Figure 94 displays a tentative correlation of these horizons between the Pine and Sukunka Rivers. The possibility exists that these bentonites correlate with those discussed earlier along the Peace River. These correlations are strongly influenced by the distinctive nature of the Bluesky (N) unit (Kilby, 1984a). This unit is persistent from the Peace River to south of the Sukunka River. The three members of the unit from the base up are: a thin conglomerate or conglomeratic unit; a turbiditic, coarsening-up, bioturbated, silty mudstone; and a glauconitic mudstone or glauconite sand interval. This unit is readily distinguishable in boreholes and well-exposed outcrop sections. In the south it is overlain by the Upper Gething and forms the basal part of the Moosebar Marine tongue of Duff and Gilchrist (1981).

The Fisher Creek Tonstein zone (Kilby, 1984b) was traced both northward and southward (Fig. 95). Examination of the Gething section along Moosebar Creek yielded a fault repeated occurrence of the Fisher Creek Tonstein whose identity was confirmed by the presence of the No. 2 Tonstein 30 metres stratigraphically below it; Kilby (1984b, Fig. 38b) suggested this possibility. Examination of borehole geophysical and lithological logs from the Sukunka and Quintette areas indicates the presence of tonsteins in the proper position to match the Fisher Creek and No. 2 intervals. The Gething Formation north of Burnt-Sukunka Rivers is equivalent to the Lower Gething of the Sukunka region. The Upper Gething of the Sukunka area contains locally well-known coal seams such as the Bird, Chamberlain, and Skeeter; it has no expression north of the Burnt-Sukunka area. The Fisher Creek Tonstein, No. 2 Tonstein, and Bluesky (N) are all parallel and approximately 30 metres apart over the Peace to Sukunka River area. This association is very useful in correlating sections from the many properties. It can now be shown that the following seams were being deposited at the time the Fisher Creek Tonstein fell: Trojan Seam in the Peace River area; No. 1 Seam at Willow Creek; E Seam at Noman Creek; Brenda Seam at Falling Creek; No. 1 Seam at Goodrich; and B Seam at Sukunka.

Excellent exposures of the Bluesky (N) and Fisher Creek Tonstein zone occur on an exploration road along Chamberlain Creek. The Fisher Creek Tonstein was sampled for radiometric age dating along Fisher Creek and is presently being processed. This data and those obtained from the

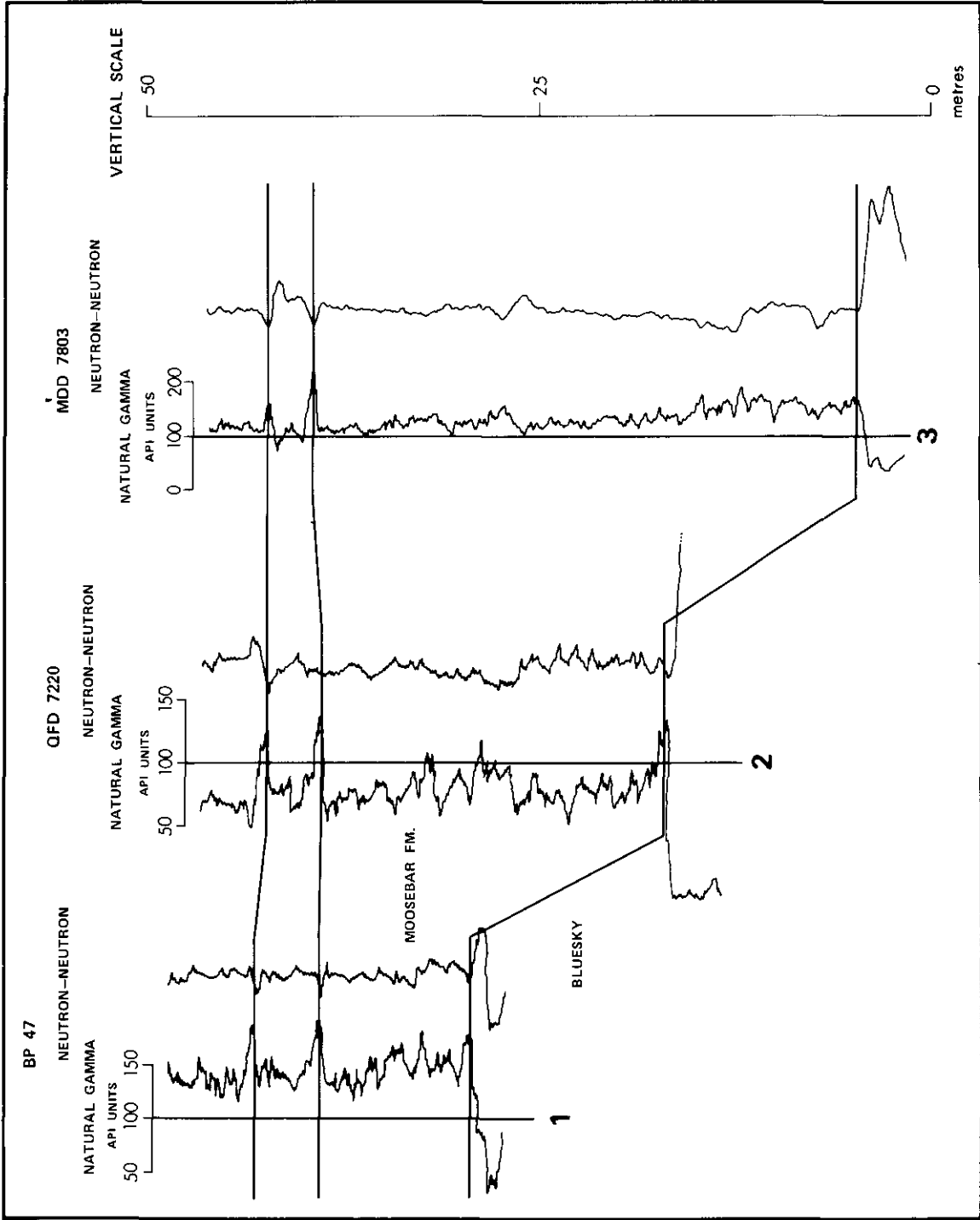


Figure 93. Twin bentonite horizons and the Gething-Moosebar formational contact. See Figure 90 for location.

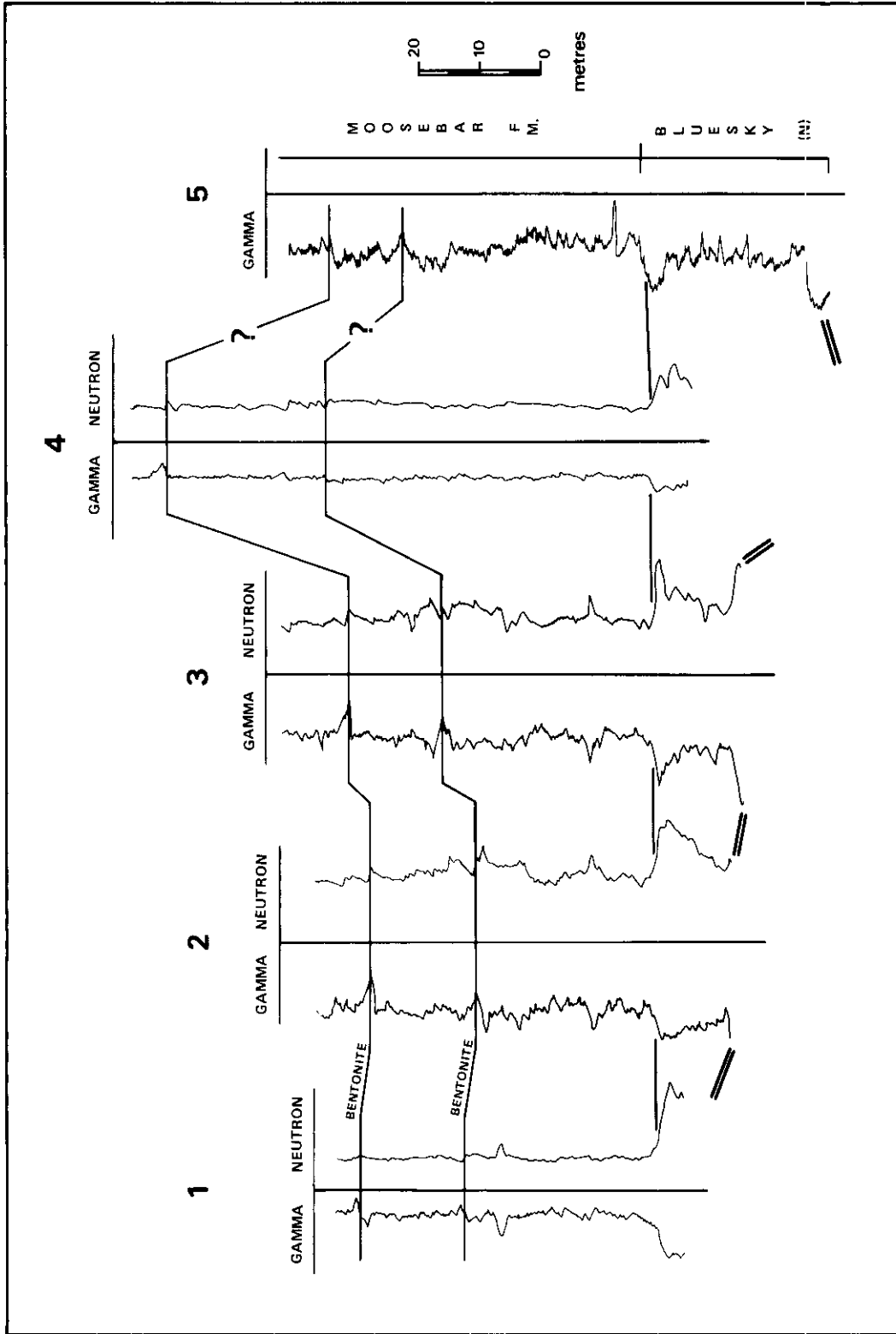


Figure 94. Borehole geophysical traces of the lower Moosebar to Bluesky interval north of the Sukunka River area. Column 4 is exaggerated due to bedding to core angles of 50 degrees. See Figure 90 for location.

TABLE 1  
ANALYSES OF 58 TONSTEIN SAMPLES

| SAMPLE | FORMATION | SI02  | AL2O3 | FE2O3 | MGO  | CAO   | NA2O  | K2O  | TI02  | MNO   | P2O5 | Rb  | Sr  | Zr  |
|--------|-----------|-------|-------|-------|------|-------|-------|------|-------|-------|------|-----|-----|-----|
| R82-1  | MOOS      | 37.72 | 21.76 | 4.0   | 4.15 | 9.94  | .10   | .32  | .61   | .035  | .35  | <5  | 160 | 108 |
| R82-2  | MOOS      | 49.98 | 27.62 | 2.31  | .99  | 2.39  | .35   | 1.6  | .77   | .006  | .48  | 22  | 264 | 57  |
| R82-3  | MOOS      | 43.68 | 35.07 | 2.91  | <.11 | 1.14  | .12   | .15  | .64   | .01   | .96  | <5  | 642 | 105 |
| R82-4  | MOOS      | 21.79 | 15.69 | 7.28  | 7.67 | 17.41 | .1    | .1   | .46   | .051  | .23  | <5  | 197 | 43  |
| R82-5  | GETH      | 44.97 | 36.64 | .05   | .15  | .12   | .14   | .3   | .88   | .004  | .02  | <5  | 43  | 36  |
| R82-6  | GETH      | 45.69 | 33.0  | .12   | <.11 | <.09  | .14   | .28  | 1.05  | <.002 | .02  | <5  | 46  | 103 |
| R82-7  | MOOS      | 46.16 | 32.63 | 3.62  | .65  | 1.83  | .21   | .51  | .76   | .023  | .82  | <5  | 270 | 260 |
| R82-8  | GETH      | 47.17 | 34.83 | 1.73  | .2   | .62   | .09   | .15  | 1.17  | .013  | .45  | <5  | 267 | 105 |
| R82-9  | GETH      | 52.66 | 22.7  | 1.51  | 1.71 | 3.78  | 1.81  | .51  | .89   | .02   | .02  | <5  | 189 | 97  |
| R82-10 | GETH      | 39.04 | 23.06 | 3.22  | 3.95 | 6.83  | .44   | 1.34 | .71   | .034  | .02  | 20  | 104 | 68  |
| R82-11 | MOOS      | 25.94 | 19.71 | 5.84  | 6.27 | 14.86 | .1    | .16  | .52   | .037  | .53  | <5  | 434 | 185 |
| R82-12 | GETH      | 52.56 | 18.21 | 1.46  | 2.12 | 4.26  | 1.14  | 3.2  | .52   | .008  | .04  | 32  | 100 | 158 |
| R82-13 | GETH      | 48.73 | 25.79 | 1.53  | 1.67 | 2.68  | 0.43  | 5.16 | .7    | .015  | .02  | 32  | 62  | 75  |
| R82-14 | GETH      | 40.34 | 22.23 | 2.51  | 2.81 | 5.07  | 0.48  | 0.88 | .69   | .03   | .02  | 14  | 83  | 120 |
| R82-15 | GETH      | 52.55 | 26.35 | 2.36  | 1.93 | 0.2   | 1.37  | 1.77 | .81   | .021  | .02  | 22  | 85  | 213 |
| R82-16 | GETH      | 52.45 | 23.54 | 3.04  | 2.96 | 0.58  | 1.92  | 1.52 | .73   | .026  | .03  | 20  | 111 | 135 |
| R82-17 | GETH      | 47.87 | 25.47 | 2.06  | 1.52 | 1.96  | 0.37  | 3.83 | .72   | .02   | .02  | 33  | 58  | 95  |
| R82-18 | GETH      | 51.01 | 26.63 | 1.16  | 1.54 | 3.0   | 0.83  | 0.42 | 1.015 | .014  | .05  | <5  | 186 | 260 |
| R82-20 | GETH      | 49.36 | 33.82 | 1.11  | 0.18 | 0.19  | 0.02  | 0.31 | 1.26  | .01   | .16  | 9   | 330 | 337 |
| R82-21 | GETH      | 51.15 | 34.03 | 0.05  | <.11 | <.09  | 0.02  | 0.06 | 1.13  | .004  | .08  | <5  | 300 | 156 |
| R82-22 | GETH      | 49.86 | 26.42 | 1.03  | 1.48 | 1.86  | 1.22  | 0.98 | .79   | .014  | .02  | 9   | 114 | 184 |
| R82-23 | GETH      | 50.98 | 34.62 | 0.15  | <.1  | 0.11  | 0.01  | 0.08 | 1.07  | .003  | .11  | <5  | 66  | 168 |
| R82-24 | GETH      | 52.04 | 21.76 | 0.26  | <.11 | 0.12  | 0.03  | 0.29 | 1.95  | <.002 | .07  | <5  | 645 | 73  |
| R82-25 | GETH      | 44.89 | 35.27 | 0.09  | 0.22 | 0.15  | 0.16  | 0.25 | .91   | <.002 | .02  | <5  | 103 | 30  |
| R82-26 | GETH      | 53.07 | 27.78 | 0.62  | 0.70 | 1.86  | 1.28  | 0.34 | .96   | .003  | .03  | <5  | 103 | 232 |
| R82-27 | GETH      | 54.11 | 27.67 | 0.8   | 0.72 | 0.98  | 1.45  | 0.53 | .77   | .011  | .02  | <5  | 213 | 102 |
| R82-28 | GETH      | 39.49 | 25.11 | 4.88  | 2.61 | 4.96  | 1.29  | 1.18 | .8    | .34   | .07  | 22  | 161 | 144 |
| R82-29 | GETH      | 51.44 | 24.87 | 1.6   | 0.92 | 1.82  | 0.549 | 4.94 | .57   | .012  | .02  | 55  | 95  | 57  |
| R82-30 | GETH      | 53.25 | 27.38 | 0.66  | 0.75 | 1.18  | 0.24  | 1.10 | .70   | .003  | .02  | 7   | 167 | 50  |
| R82-31 | GETH      | 40.47 | 27.91 | 12.07 | 0.99 | 0.8   | 0.06  | 0.74 | .75   | .097  | .29  | 10  | 260 | 54  |
| R82-32 | GETH      | 42.06 | 33.5  | 0.23  | 0.07 | 0.34  | 0.05  | 0.31 | .43   | <.003 | .02  | <5  | 167 | 26  |
| R82-33 | GETH      | 50.   | 30.79 | 3.67  | 0.09 | 0.42  | 0.09  | 0.44 | .7    | .017  | .24  | 9   | 237 | 45  |
| R82-34 | GETH      | 41.33 | 23.56 | 0.22  | 0.09 | 0.19  | 0.06  | 0.23 | .66   | <.003 | .03  | <5  | 97  | 25  |
| R82-35 | GETH      | 47.75 | 34.75 | 0.27  | 0.15 | 0.11  | 0.48  | 0.71 | 1.32  | <.003 | .03  | <5  | 205 | 31  |
| R82-36 | MOOS      | 29.63 | 23.21 | 4.46  | 4.98 | 11.86 | 0.11  | 0.21 | .56   | .024  | .79  | <5  | 300 | 551 |
| R82-37 | MOOS      | 46.34 | 32.81 | 2.42  | 0.53 | 1.86  | 0.14  | 0.72 | .59   | .011  | .65  | 12  | 138 | 406 |
| R82-38 | MOOS      | 20.52 | 14.31 | 6.04  | 8.92 | 18.42 | 0.06  | 0.12 | .27   | .049  | .21  | <5  | 110 | 197 |
| R82-39 | MOOS      | 37.05 | 20.84 | 7.19  | 3.67 | 8.64  | 0.08  | 0.41 | .53   | .031  | .37  | 9   | 150 | 143 |
| R82-40 | MOOS      | 42.64 | 18.95 | 6.4   | 3.24 | 7.51  | 0.15  | 1.31 | .49   | .023  | .33  | 21  | 90  | 160 |
| R82-41 | GETH      | 53.02 | 28.92 | 1.57  | 0.94 | 0.59  | 0.6   | 0.8  | .86   | .012  | .02  | 11  | 177 | 58  |
| R82-42 | GETH      | 33.86 | 22.12 | 4.83  | 4.36 | 9.55  | 0.73  | 0.51 | .87   | .051  | .33  | <5  | 127 | 88  |
| DUP-23 | ●         | 50.29 | 35.07 | .14   | <.06 | .26   | .02   | .11  | .92   | .004  | .12  | <5  | 73  | 172 |
| DUP-35 | ●         | 47.92 | 34.58 | .27   | .09  | .1    | .47   | .69  | 1.31  | <.003 | .03  | <5  | 222 | 26  |
| R83-2  | GETH      | 45.82 | 35.65 | .1    | .07  | .28   | .08   | .08  | .45   | <.003 | ●    | 10  | 15  | 270 |
| R83-3  | GETH      | 43.24 | 36.48 | .15   | <.06 | .91   | .09   | .24  | .84   | <.003 | ●    | 10  | 27  | 138 |
| R83-5  | GETH      | 39.71 | 26.71 | 16.07 | .26  | .35   | .16   | .27  | .59   | .085  | ●    | <10 | 32  | 185 |
| R83-6  | GETH      | 36.75 | 26.19 | 4.51  | 2.93 | 7.83  | .06   | .38  | .6    | .031  | ●    | 14  | 320 | 160 |
| R83-7  | GETH      | 38.44 | 25.26 | 16.55 | .16  | .08   | .1    | .27  | .68   | .038  | *    | 15  | 27  | 185 |
| R83-8  | GETH      | 48.53 | 34.1  | .74   | .16  | .32   | .38   | .77  | 1.27  | .004  | ●    | 15  | 30  | 312 |
| R83-9  | GETH      | 49.8  | 33.31 | .78   | .1   | .37   | .06   | .54  | .85   | .006  | ●    | 13  | 33  | 152 |
| R83-10 | GETH      | 51.07 | 33.41 | .12   | .07  | .13   | .06   | 1.08 | 1.07  | <.003 | *    | 13  | 22  | 312 |
| R83-11 | GETH      | 45.77 | 29.93 | 8.36  | .18  | .27   | .08   | .35  | .82   | .058  | ●    | 15  | 32  | 200 |
| R83-13 | GETH      | 49.3  | 33.72 | .26   | .1   | .45   | .04   | .37  | .68   | <.003 | ●    | 10  | 95  | 200 |
| R83-14 | GETH      | 45.01 | 31.34 | 7.54  | .2   | .28   | .04   | .34  | .85   | .4    | ●    | 13  | 21  | 223 |
| R83-15 | GETH      | 48.23 | 35.25 | .36   | .07  | .64   | .06   | .38  | .83   | .004  | ●    | 10  | 30  | 138 |
| R83-20 | GETH      | 46.14 | 32.48 | 3.58  | .2   | .79   | .06   | .28  | 1.01  | .028  | ●    | 11  | 100 | 152 |
| R83-24 | GETH      | 37.05 | 24.8  | 4.75  | 3.6  | 6.25  | .2    | .28  | .83   | .041  | ●    | 15  | 63  | 132 |
| R83-25 | GETH      | 51.7  | 27.91 | 1.44  | .79  | 1.08  | .33   | 2.64 | .62   | .007  | ●    | 32  | 100 | 127 |
| R83-26 | GETH      | 50.18 | 24.78 | 2.58  | .81  | 1.37  | .64   | 1.24 | .68   | .009  | ●    | 31  | 132 | 177 |
| R83-27 | GETH      | 47.41 | 30.36 | 8.52  | .24  | .26   | .08   | .35  | .83   | .061  | ●    | 14  | 45  | 135 |

bentonites in the lower Hulcross Formation may provide clues to the source area of the ash and will provide the opportunity to examine the sedimentation rates of intervening strata over a large area. The parallel character of the Gething Formation tonsteins, Bluesky (N), and the bentonites in the lower Moosebar Formation between the Peace and Sukunka Rivers indicates that the whole area was a continuous coastal swamp which was inundated virtually simultaneously over this length during the initial transgressive phases of the Clearwater Sea.

## CHEMISTRY

Assessing the potential of chemically correlating the tonsteins was one of the main objectives of the overall project. It was hoped that some means of chemically 'fingerprinting' the various altered ash bands would be found to enable rapid correlation of these horizons when new bands were encountered during exploration. At the end of the field season analytical results became available for a set of 58 samples from the 1982 and 1983 field seasons. These analyses were examined graphically and statistically using a micro-computer. The samples were from the Gething and Moosebar Formations; all were from the Pine River to Brazion Creek region. Preliminary analysis of this data is presented here and a few examples of the correlation potential based on sample chemistry also are given. Analyses for thirteen elements were performed. Si, Al, Fe, Mg, Ca, Na, K, Ti, and Mn were determined using Atomic Absorption Spectroscopy techniques. Samples were prepared by fusion in borate glass crucibles, fluoro-borate dissolution, and stabilization of silica. The A.A.S. unit was calibrated using synthetic multi-element standards; the data were reduced on a micro-computer using least squares poly-sensitivity drift monitoring and correction, and a weighted least squares fit calculation for calibration and variance. P, Rb, Sr, and Zr values were determined using X-Ray Fluorescence instrumentation. The lanthanum doped borate glass method was employed using natural standards with line overlap mathematical corrections. All sample preparation and testing were performed by personnel of the Ministry of Energy, Mines and Petroleum Resources Analytical Laboratory. Results of the 58 samples are presented in Table 1. These data were entered into a micro-computer and stored using the Data Handler module of the Cal Data Geological Analysis Package. Most software utilized in the study was contained in the Statistical and Geochemical modules of this package but several programs were written by the author to perform specific procedures. Correlation coefficients between the 13 elements were calculated to examine tendencies of certain element abundances to be mirrored by other elements. Significant positive and negative correlations are highlighted in the correlation coefficient matrix (Fig. 96a). The significances of the matrix values were based on a student's t-test with 11 degrees of freedom at a confidence level of 99 per cent. Positive correlations indicate that as one variable increases or decreases the corresponding element does the same. A negative value means as one element increases or decreases in abundance the corresponding element does the reverse. A

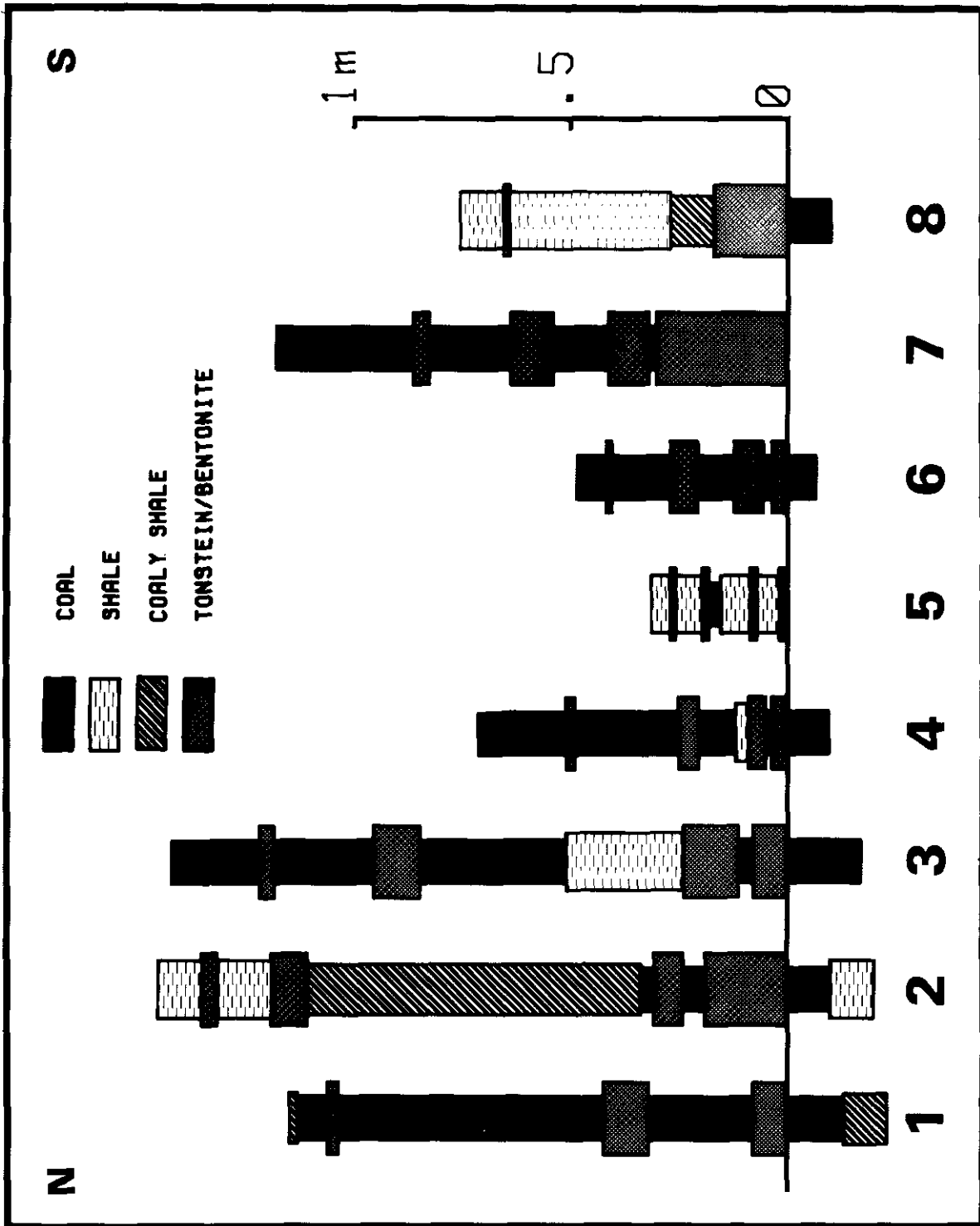


Figure 95. Detailed sections of the Fisher Creek tonstein zone from widely spaced borehole and outcrop locations. See Figure 90 for location.

dendrogram of the matrix was used to graphically illustrate the correlations between elements (Fig. 96b). The strong correlation between Ca and Mg suggests that these elements are related to a common source which would be the secondary carbonates: dolomite, calcite, and magnesite. Mg and Ca have strong negative correlation coefficients with Si and Al, the two most abundant elements. This relationship and the identification of carbonates in many of the samples, by microscopic and XRD methods, suggest that the carbonates were diagenetic. Figure 97 is a ternary plot of SiO<sub>2</sub>/Al<sub>2</sub>O<sub>3</sub>/CaO abundances. The mean SiO<sub>2</sub> to Al<sub>2</sub>O<sub>3</sub> ratio is about 1.66:1; the CaO content appears to be completely independent of their concentrations because various concentrations of CaO do not affect the SiO<sub>2</sub>:Al<sub>2</sub>O<sub>3</sub> ratio. Two groups are suggested on the diagram: one contains those samples which were affected by the introduction of carbonate, the other group containing samples which were unaffected by the secondary introduction of carbonate. Samples which showed an increase in carbonate content were found in both the Moosebar and Gething Formations. A plot of TiO<sub>2</sub> versus Zr was used to determine the likely original composition of the ash prior to alteration. The plot follows a procedure similar to Spears and Duff (1984) (Fig. 98). The values were normalized to 15 per cent Al<sub>2</sub>O<sub>3</sub>. The original ash compositions suggested by this plot were in the andesite to rhyolite range (Winchester and Floyd, 1977). Using these derived original compositions the mean SiO<sub>2</sub>:Al<sub>2</sub>O<sub>3</sub> ratios for andesite and rhyolite are about 4.5:1; average of samples of Mount St. Helens ash had a ratio of 3.5:1. Thus the average tonstein ratio of 1.66:1 indicates that the major chemical affect of alteration was a net loss of silica from the ash bands. The downward migration of silica from bentonites is not uncommon (Grim and Guven, 1978). The strong correlation coefficient between K<sub>2</sub>O and Rb is believed to reflect the substitutability of these two elements due to their similar ionic charges and radii.

Correlation of these tonstein samples on the basis of chemistry was attempted by a form of cluster analysis based on similarity coefficients. The similarity coefficient employed had been used successfully to chemically correlate recent volcanic ash horizons (Sarna-Wojcicki, *et al.*, 1984). The coefficient was obtained by calculating the average of the ratios of corresponding elements from the two samples being compared. The denominator was always larger than the numerator in the ratios because the maximum ratio obtainable was 1.0. Eleven elements were used in the calculation, P<sub>2</sub>O<sub>5</sub> and Rb were excluded because a significant number of samples were not analysed or were below detection limit for these elements. Element abundances were normalized to 100 per cent in an effort to remove the effect of variable amounts of included organic material which had no expression in the chemical results. Element abundances reported as less than the detection limit arbitrarily were given the value of one half the detection limit. A symmetrical 60 by 60 matrix of similarity coefficients was produced; the two extra samples were laboratory duplicates included to show the sensitivity of the procedure. Information contained in the similarity matrix has been summarized in the form of a dendrogram produced using the weighted pair-



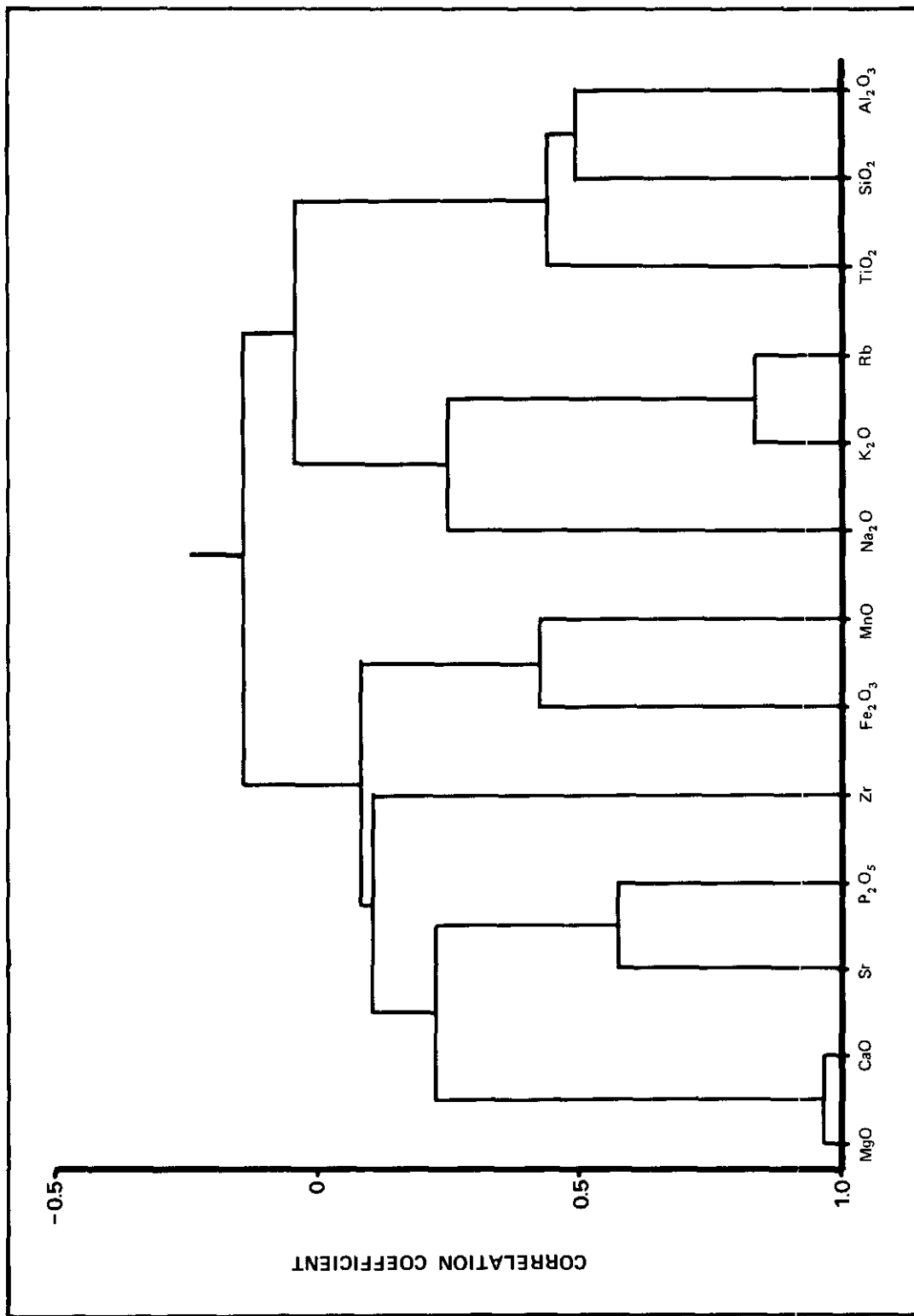


Figure 96b. (b) Dendrogram constructed from the correlation coefficient matrix by the weighted pair-group clustering method.

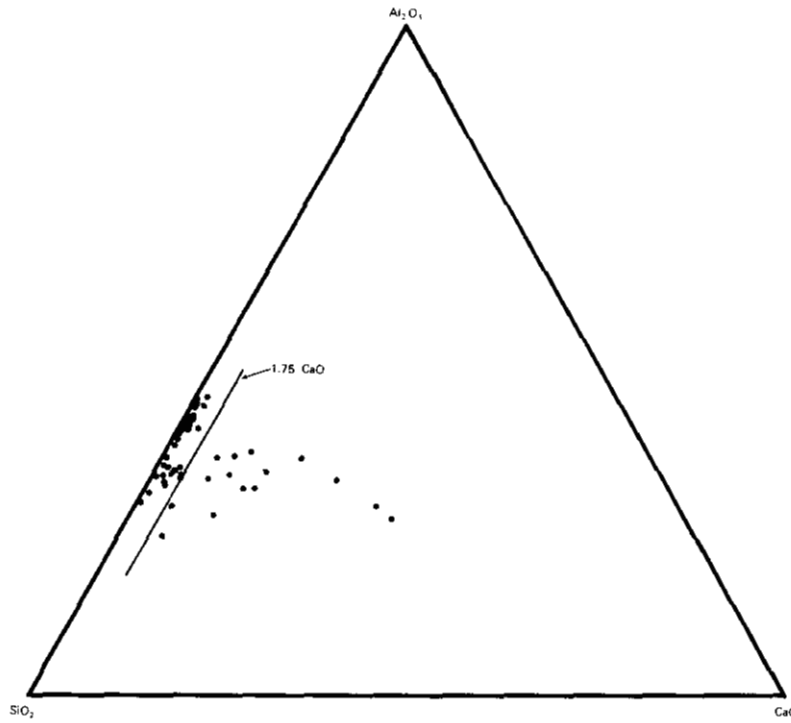


Figure 97. Ternary plot of  $\text{SiO}_2/\text{Al}_2\text{O}_3/\text{CaO}$  for all 58 samples. Note the consistent  $\text{SiO}_2/\text{Al}_2\text{O}_3$  ratio about 1.66:1 which does not vary as the percentage of CaO changes.

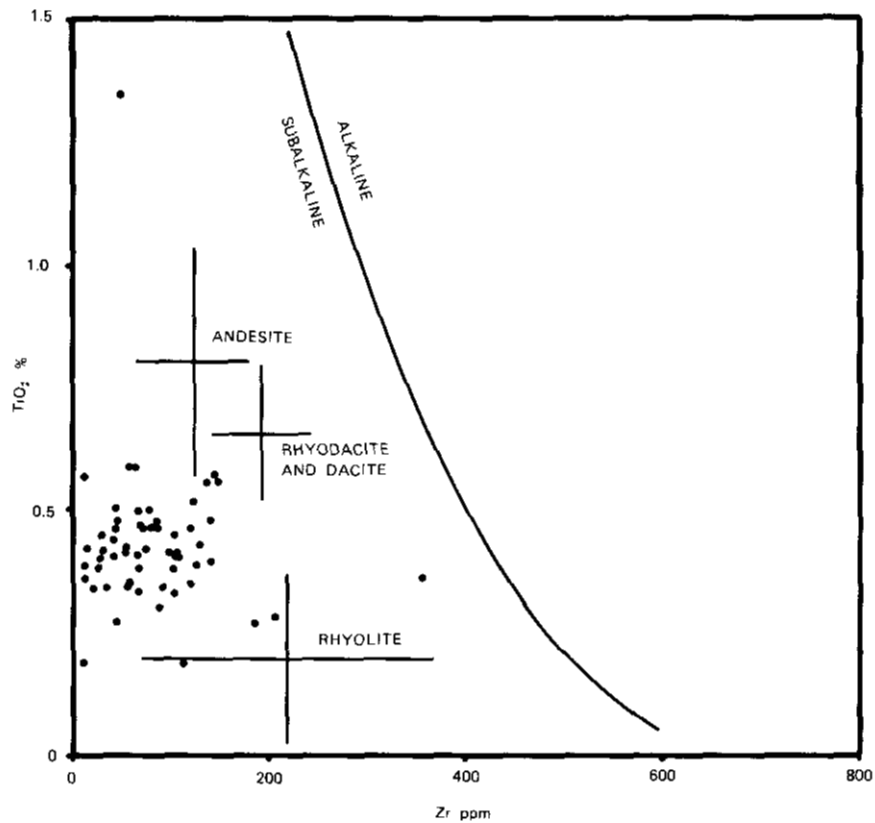


Figure 98.  $\text{TlO}_2$  versus Zr plot (Spears and Duff, 1984); for reference, average ratios for andesite, rhyolite, and rhyodacite are indicated (Winchester and Floyd, 1977). Values are normalized to 15 per cent  $\text{Al}_2\text{O}_3$ .

group average clustering technique (Fig. 90). The geological relationships of samples with high similarity coefficients were investigated. The similarity coefficient calculations did not take into account the relative proportions of various elements in each sample; therefore a difference of 25 per cent to 50 per cent SiO<sub>2</sub> would have the same effect on the similarity coefficient as a 0.02 per cent to 0.04 per cent CaO difference. Thus when interpreting the similarity coefficients care must be used, absolute values are not as important as the relative values for each sample. An example of this problem is demonstrated by the relatively low similarity coefficient between R82-23 and the duplicate of this sample, DUP-23. This difference between identical samples was due to the CaO and Na<sub>2</sub>O values (Table 1). The difference between the Na<sub>2</sub>O values is well within one standard deviation of the analysis technique and the CaO values are approximately one standard deviation apart. More sophisticated correlation techniques will be performed on this data but even within the limitations of the present method individual horizons could be chemically correlated.

Two boreholes, approximately 2 kilometres apart, drilled through the lower Moosebar Formation intersected similarly positioned bentonite horizons (Fig. 100). In this example three pairs of bentonites were strongly correlated; they had the highest mutual similarities which formed primary linkages on the dendrogram. Samples R82-39 and R82-40 had a high similarity coefficient, 0.76; there was no horizon corresponding with R82-40 located in hole 1 which led to the geological interpretation that R82-39 and R82-40 were from the same band which had been structurally repeated in hole 2. It was encouraging that the chemical correlation connected horizons that were geologically acceptable and explained the lack of a corresponding layer to match the R82-40 layer.

Correlation of tonsteins by the method of similarity coefficient matrix examination provided the solution to a confusing series of Gething Formation coal intersections and tonsteins in a borehole (Fig. 101). Similar responses outlining coal seams on the Detailed Sidewall Density trace and chemical correlations of the tonsteins demonstrated which sections were repeats and suggested the locations of the intervening faults. Coal seams A, B, and C are believed to represent an undisturbed section and include four tonsteins. These four tonsteins are believed to be the Fisher Creek Tonstein zone (Fig. 95). Coal intervals A and F are interpreted to be fault duplicates on the basis of the seam density trace and the strong correlations between samples R82-10 and R82-14, and R82-13 and R82-17. Intervals B and C are correlated with intervals D and E on the basis of the density traces and a good correlation between R82-15 and R82-15. Two faults are required to arrive at this configuration of seams and their approximate positions are given on Figure 101. An example of seam correlation between different exposures on the basis of tonsteins is also given on Figure 101. Samples R82-28 and R82-29 correlate with the lower two tonsteins in the undisturbed portion of the borehole section. The uppermost tonstein in the trench, R82-25, correlates with R82-5 and R82-6, the uppermost tonsteins in the two duplicated upper portions of

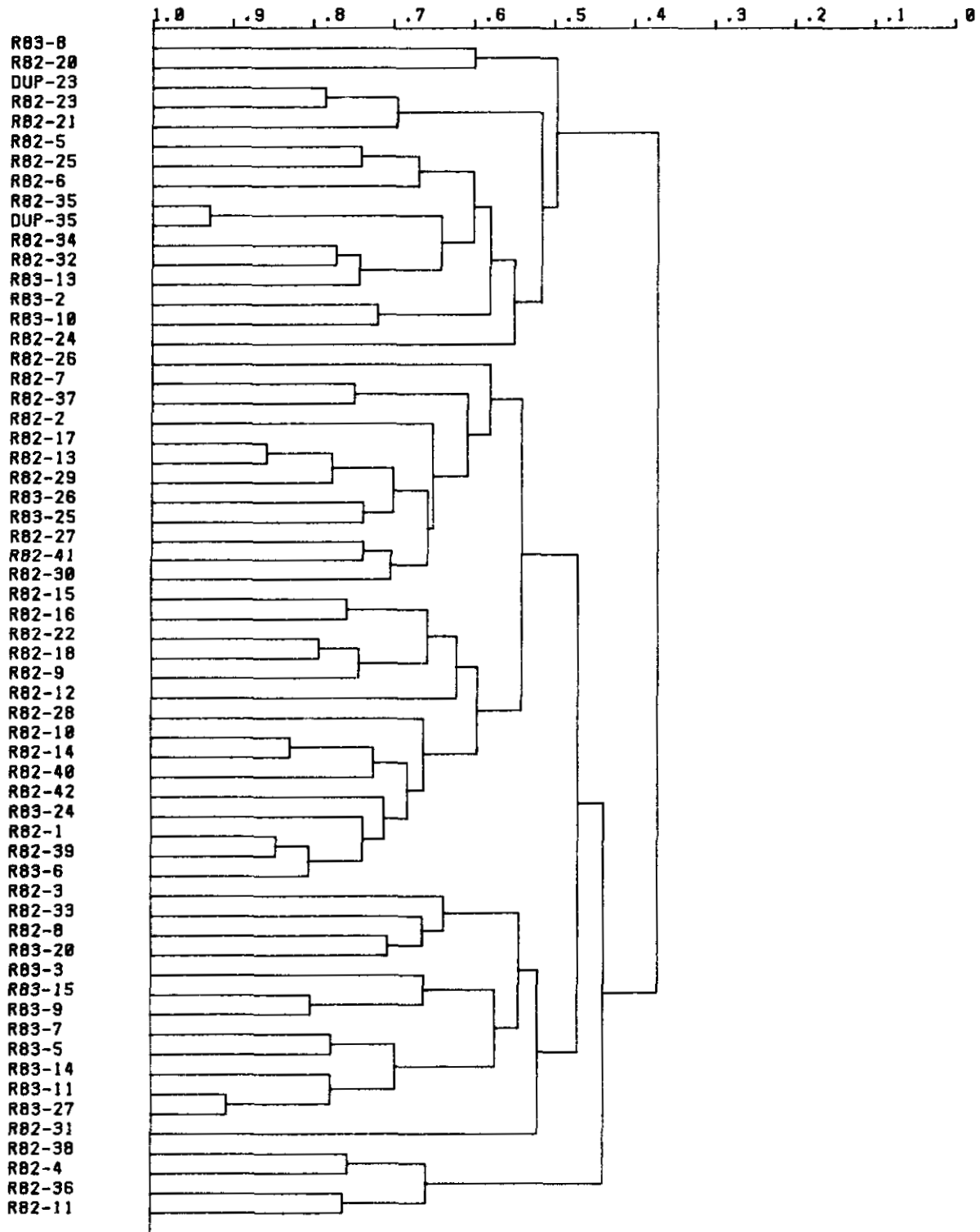


Figure 99. Similarity coefficient dendrogram of 60 samples calculated by the weighted pair-group clustering technique. Two duplicate samples (DUP-) are included to illustrate the sensitivity of the method.

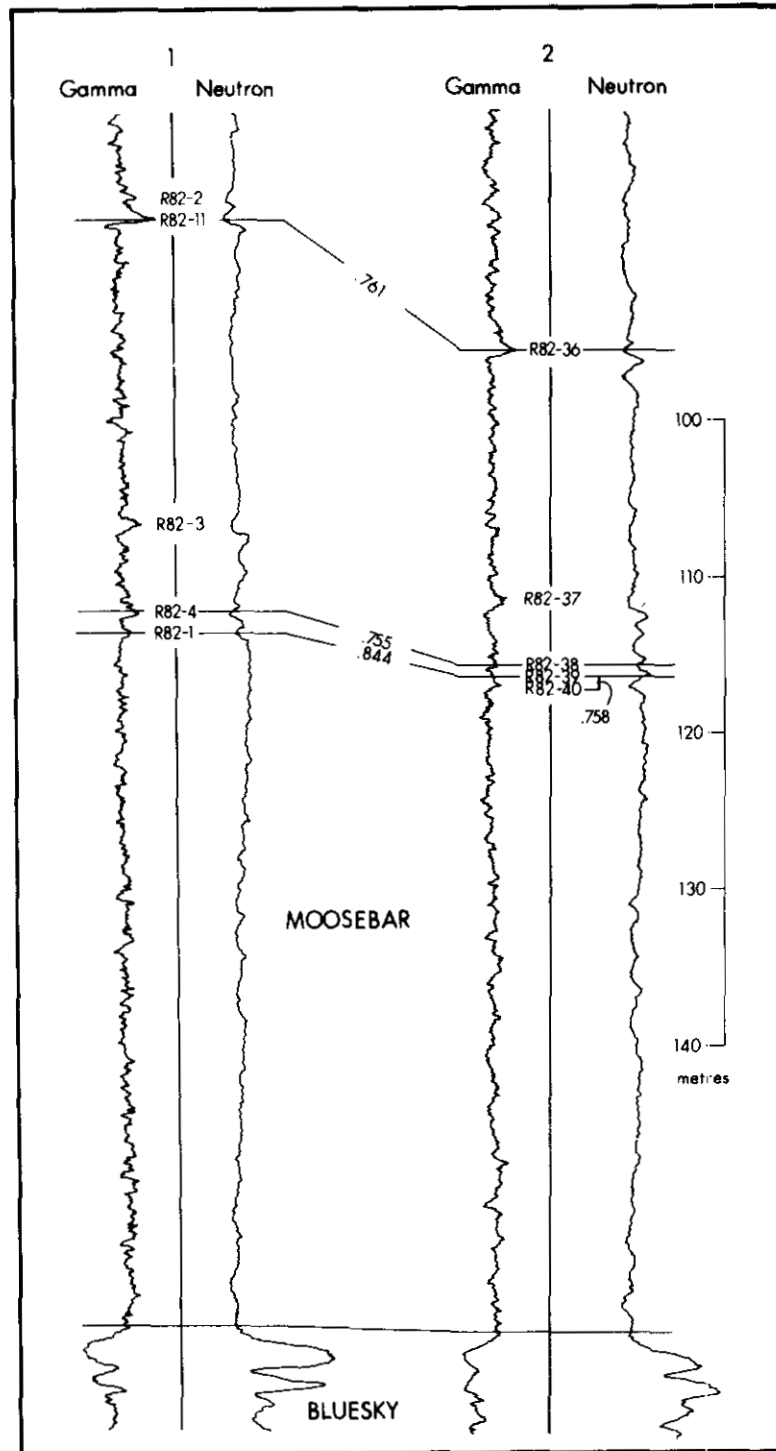


Figure 100. Geophysical logs from two borehole sections of the lower Moosebar and Bluesky sequences. Sample numbers denote the positions of ash bands. Bold correlation lines indicate primary linkages on Figure 99.

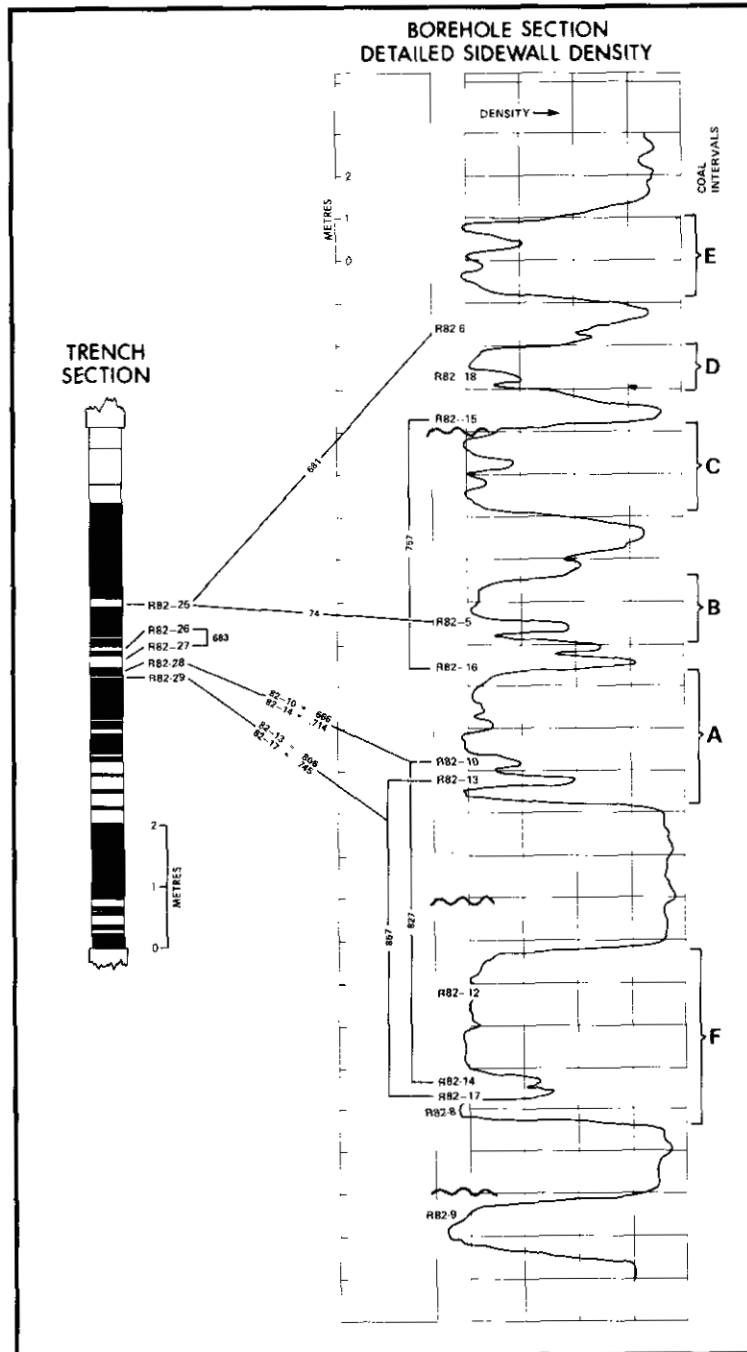


Figure 101. Correlation example from a Gething Formation coal zone. A trench and borehole section are correlated on the basis of similarity coefficients. The fault locations and seam duplications were determined by examination of the geophysical log trace and similarity coefficients. Dashed correlation lines indicate correlations with high similarity coefficients but not the mutually highest coefficients between the two samples.

the coal sequence in the borehole section. Samples R82-26 and R82-27 appear to be one repeated band. The apparent thickness difference between these two sections is due to the bedding-to-core angle in the borehole. This is an excellent illustration that near surface weathering encountered in the trench did not significantly effect the trench samples. The second strongest similarity coefficient (Fig. 99), between samples R83-11 and R83-27, represented correlations between suspected Fisher Creek Tonsteins located approximately 15 kilometres apart. Chemical correlation appears very promising, even using the simplest of statistical techniques. Many of the correlations suggested on the similarity coefficient dendrogram are geologically acceptable but have not yet been explored in detail.

### **MINERALOGICAL**

Mineralogical correlation was attempted on the basis of X-Ray diffractograms. Visual examination of the diffractograms of samples which were correlated geologically and chemically showed strong similarities (Fig. 102). In this example two tonsteins located within 2 metres of each other stratigraphically are fault repeated in a borehole (Fig. 101). Diffractograms from the four samples show different mineralogy between the two bands but similar mineralogy between corresponding tonsteins across the fault; strong chemical similarities also exist between these two pairs of samples. It is important to note that even with obviously different mineralogy, similarity coefficients are relatively high between the two bands (R82-16 to R82-14 = 0.748). A combination of chemical and mineralogical correlation may prove to be the most effective approach. This type of correlation is in its initial stages, an automated technique is now under development and should provide relatively fast and cost effective measures of similarity analysis.

### **CONCLUSION**

Work on the Tonstein-Bentonite study during 1984 has: (1) extended the correlation distance of several of the previously described altered ash horizons; (2) initiated age dating of these horizons; (3) shown the ability of chemistry and mineralogy to distinguish specific tonstein-bentonite horizons over limited areas. Future work on this project will be directed to extending correlations of the ash bands, investigating more sophisticated chemical and mineralogical correlation techniques, and documenting stratigraphic relationships relative to these time lines.

### **ACKNOWLEDGMENTS**

The author would like to thank members of the active exploration companies in the area of this study: Gulf Canada Resources Inc., Crows

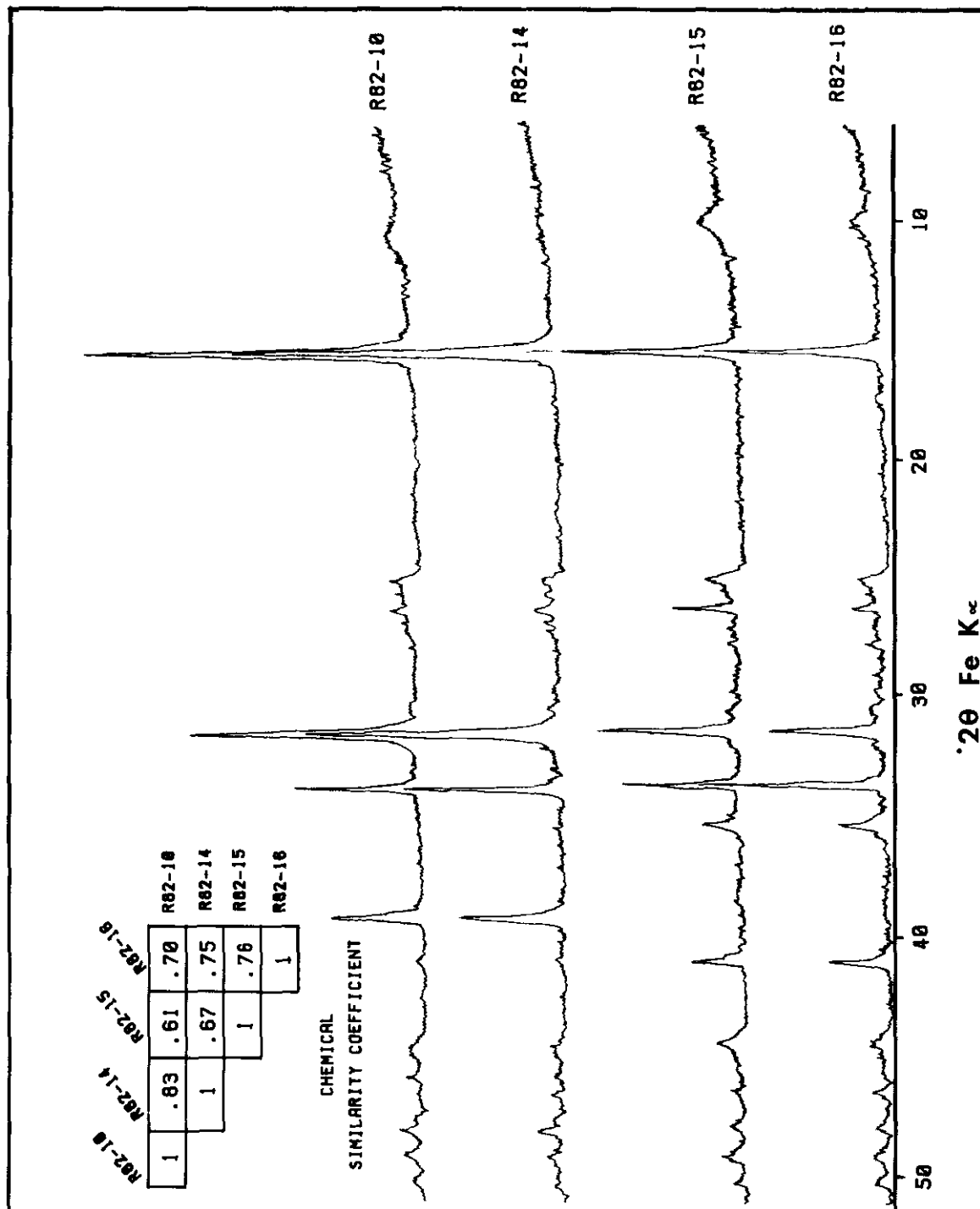


Figure 102. Example of X-ray diffractograms of four tonsteins illustrated on Figure 101. The chemical similarity coefficients are given in matrix form to provide a comparison between mineralogical and chemical similarities. The XRD measurement rate was  $2\phi$ /min and samples were bombarded with FeK $\alpha$  radiation.

Nest Resources Ltd., and Esso Resources Canada Ltd. Their aid in locating occurrences of these ash horizons, access to newly obtained drill core, and stimulating discussion were greatly appreciated.

#### REFERENCES

- Duff, P.McL.D. and Gilchrist, R. D. (1983): Correlation of Lower Cretaceous Coal Measures, Peace River Coalfield, British Columbia, B.C. Ministry of Energy, Mines & Pet. Res., Paper 1981-3, 31 pp.
- Grin, R. E. and Guven, N. (1978): Bentonite - Geology, Mineralogy, Properties and Uses, Development in Sedimentology, Elsevier, No. 24, 256 pp.
- Kilby, W. E. (1984a): The Character of the Bluesky Formation in the Foothills of Northeastern British Columbia (930, P, I), B.C. Ministry of Energy, Mines & Pet. Res., Geological Fieldwork, 1983, Paper 1984-1, pp. 109-112.
- ..... (1984b): Tonsteins and Bentonites in Northeast British Columbia (930, P, I), B.C. Ministry of Energy, Mines & Pet. Res., Geological Fieldwork, 1983, Paper 1984-1, pp. 95-107.
- Sarna-Wojcicki, A. M., Bowman, H. R., Meyer, C. E., Russell, P. C., Woodward, M. J., McCoy, G., Rowe, J. J. Jr., Baedecker, P. A., Asaro, F., and Michael, H. (1984): Chemical Analyses, Correlations, and Ages of Upper Pliocene and Pleistocene Ash Layers of East-Central and Southern California, U.S. Government Printing Office, Geological Survey Professional Paper 1293.
- Spears, D. A. and Duff, P.McL.D. (1984): Kaolinite and Mixed-layer Illite-smectite in Lower Cretaceous Bentonites from the Peace River Coalfield, British Columbia, *Can. Jour. Earth Sci.*, Vol. 21, pp. 465-476.
- Winchester, J. A. and Floyd, P. A. (1977): Geochemical Discrimination of Different Magma Series and their Differentiation Products using Immobile Elements, *Chemical Geology*, 20, pp. 325-343.

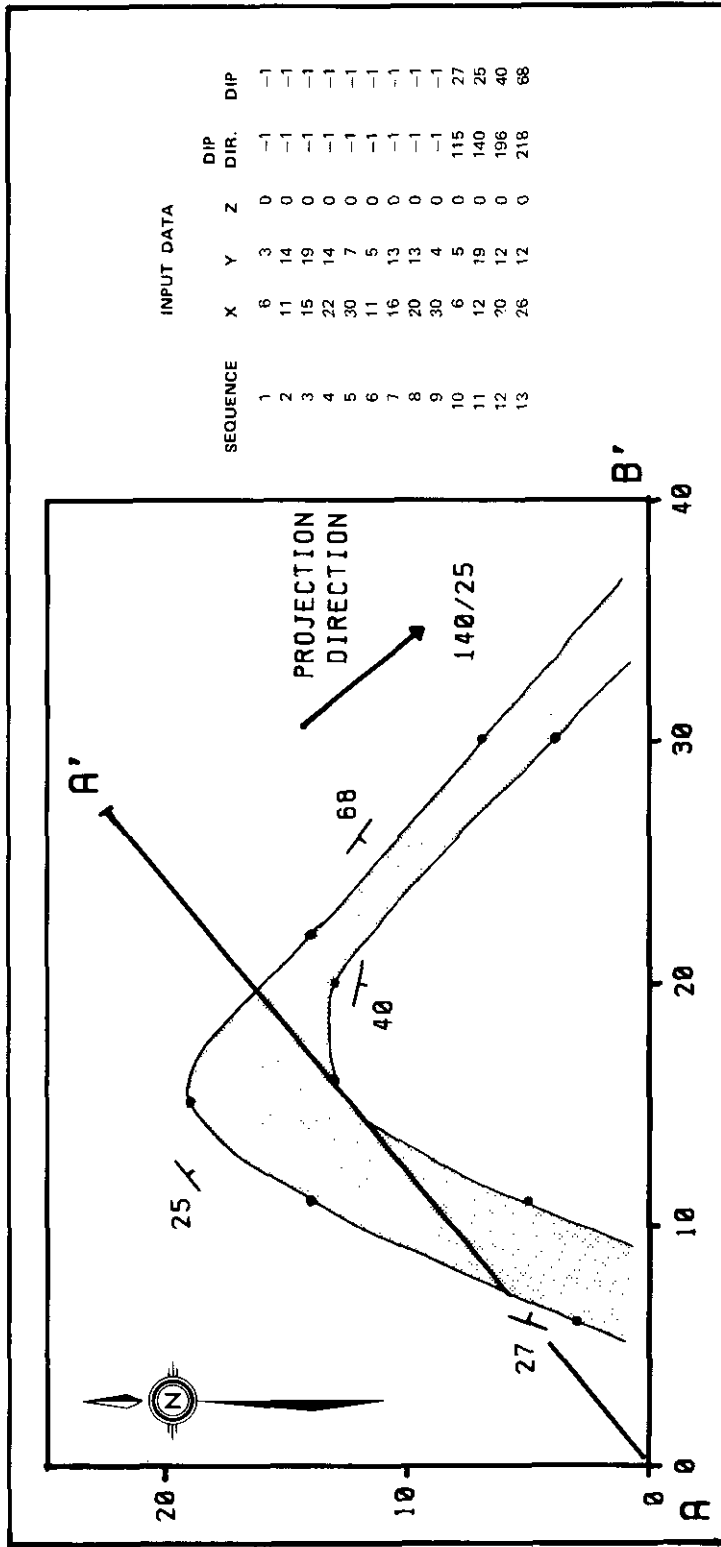


Figure 103. Hypothetical geologic map data. The figure consists of a map view showing a syncline plunging to the southeast and a table with numerical equivalents of the data displayed on the map. Note section lines A-A' and A-B'.